2011 50th IEEE Conference on Decision and Control and
European Control Conference (CDC-ECC)
Orlando, FL, USA, December 12-15, 2011

Modeling and Stability Analysis of an Active Filter for DC current compensation

Giampaolo Buticchi, Luca Consolini and Emilio Lorenzani

Abstract— **The widespread use of power converters and non-linear loads connected to the grid have caused the emergence of problems regarding the power quality. Among different kind of non-linear distortion, there is the issue of the DC current component. In fact, a DC current component flowing in the grid transformers has various detrimental effects, i.e. increased harmonic distortion, increased power losses, and possible damage due to consequent overheating. This paper proposes a non-linear sensor and a compensator system that act as an active filter to remove the DC current component flowing in the power lines. In the first part, the strategy is outlined and then the stability issue is addressed by means of a simplified model. Simulation results confirmed that the simplified model closely approximates the real system. An approximated analysis of stability is also presented. Finally we present some experimental results that shows the effectiveness of the proposed solution.**

I. Introduction and problem formulation

The widespread use of power converters and non-linear loads connected to the grid have caused the emergence of problems relative to power quality.

For this purpose, international regulations have been developed to guarantee that devices connected to the grid do not deteriorate the power quality. Among different kinds of deteriorations, which can arise from non-linear distortions, there is the issue of the DC current injection/absorption, as shown in [1], [2], [3]. The DC current component can be caused by non-linear loads or by power converters, for example grid connected systems for renewable energy, AC/DC or AC/AC converters. At the moment this problem is addressed by international or country-specific regulations that impose a limit to the maximum DC current injection/absorption allowed.

However, these regulations do not guarantee that the cumulative effect of numerous power converters connected to the grid remains acceptable, without harmful effects for electric system sensitive to DC components.

The DC current component is detrimental especially for the distribution power transformers. The main effect of a DC current component flowing in a transformer is the magnetic core saturation during a sinusoidal semi-period (half-cycle saturation), see [1]. Half-cycle saturation causes an increased magnetizing current and transformer current becomes distorted with the production of a significant amount of harmonics. When operating in half-cycle saturation condition, a transformer presents an increased reactive power absorption, that implies increased power losses and, consequently, overheating, [4], [5], [6], [7]. The solution analyzed in this paper was proposed in [8] and it is applicable to single phase grid.

G. Buticchi and L. Consolini are with DII - Department of Information Engineering - University of Parma - Italy giampaolo.buticchi@nemo.unipr.it, lucac@ce.unipr.it

E. Lorenzani is with DISMI - Department of Science and Engineering Methods - University of Modena and Reggio Emilia - Italy emilio.lorenzani@unimore.it

A similar strategy was used to prevent the core saturation of the line frequency transformer used inside grid connected converters as shown in [9].

The basic idea of this solution concerns that a DC current component flowing in the power lines causes a DC voltage drop across the parasitic resistances of the power lines of the grid. This means that at the PCC (Point of Common Coupling), defined as the "interface between sources and loads on an electrical system" , there will be a small DC voltage component, which holds the information about the DC current component that is flowing through the power lines.

For this reason, removing the DC voltage component at the PCC implies setting to zero the DC current component injected by any electric devices connected at the same PCC.

The basic idea proposed in [8] could be extended to a three phase grid. In case of long transmission three phase power lines, a geomagnetic storm can induce in the wires a nearly direct DC current, causing the magnetic saturation of power transformers and electric generators with a significant heating up of coils and cores, see [10]. This heat could disable or destroy them.

This paper concerns the stability analysis of the solution proposed in [8] providing a simplified small signal model of the whole system composed by the grid, the non-linear load and the proposed solution. Simulation results verified the same behavior of the whole detailed system in comparison with the simplified model whereas the mathematical analysis proved the system stability.

This paper completes our work of [11] with some experimental results which show the effectiveness of the proposed method.

II. Operating Principle of the Proposed DC Compensation Strategy

The key element to address this problem, as shown in [8], is a very precise DC voltage sensing strategy with a high rejection ratio to the offsets usually present in the measurement chain. As a matter of fact, sensing the DC voltage drop across the parasitic resistance of the grid means extracting a DC voltage component of the order of a few hundreds of mV from a sinusoidal signal of peak-to-peak amplitude over $600V$. The detection of this small DC voltage component is realized with the use of a toroidal magnetic core with a sole winding, in the following referred to as reactor. The reactor is sized mimicking a low power toroidal transformer with a primary voltage equal to the grid one.

The operating principle resides in the asymmetric saturation of the reactor magnetic core in presence of a DC bias. In Fig. 1 is shown the reactor connected to the grid, and the current transformer used to sense the reactor's current. In this figure i_m is represents the transformer's current, i_r the reactor's current and V_{DC} the DC voltage component.

978-1-61284-799-3/11/$26.00 ©2011 IEEE

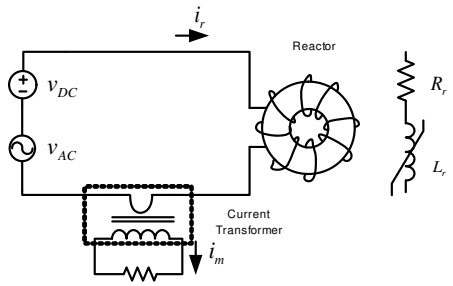

Fig. 1. Schematic of the reactor connected to the grid and the current transformer used to sense the reactor's magnetizing current.

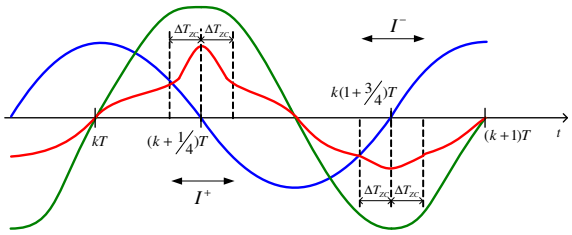

Fig. 2. Reactor voltage (blue line), magnetic flux (green line) and measured magnetizing current (red line) in presence of a positive DC bias.

Fig. 2 shows the waveforms of reactor magnetic flux and magnetizing current in presence of a positive DC voltage component v_{DC}: the magnetic flux saturates deeply at the end of the positive semi-period of the grid voltage, draining more magnetizing current. As a result, the reactor current will present a higher value in correspondence of the positive or negative grid voltage semi-period, depending on the sign of the DC voltage component. The asymmetric saturation of the magnetic core holds the information regarding both the DC voltage component sign and amplitude.

In order to obtain an offset free measurement, a current transformer is used to measure the reactor current. The transfer function between the reactor current i_r and the measured current i_m can be obtained with the model of the ideal transformer with turn ratio n, a magnetizing inductance L_m and a resistive load R_l connected at the secondary. This transfer function is given by

$$\frac{i_m(s)}{i_r(s)} = \frac{1}{n}\frac{sL_m n^2}{sL_m n^2 + R_l}\,. \tag{1}$$

Setting $p = \frac{R_l}{L_m}$, the relationship between the reactor current i_r and the sensed one i_m can be written as follows, setting $n = 1$

$$\frac{di_m}{dt} = \frac{di_r}{dt} - p\, i_m\,. \tag{2}$$

For every $k \in \mathcal{Z}$ define the two intervals

$$\begin{aligned} I_+(k) &= [k + T/4 - \Delta T_{ZC}, k + T/4 + \Delta T_{ZC}] \\ I_-(k) &= [k + 3T/4 - \Delta T_{ZC}, k + 3T/4 + \Delta T_{ZC}]\,. \end{aligned} \tag{3}$$

To detect this asymmetric distortion, during every grid voltage period, two indexes, respectively the positive saturation index (4) and the negative saturation index (5), are computed by integrating the reactor current in intervals $I_+(k)$ and $I_-(k)$, placed around voltage zero crossing, as follows

$$SI_P(k) = \int_{I_+(k)} i_m(t)\,dt \tag{4}$$

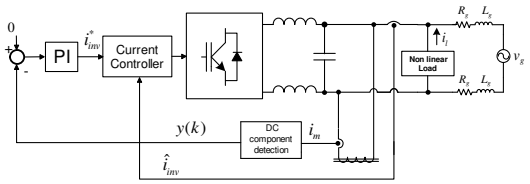

Fig. 3. Basic idea of the control scheme able to compensate the DC voltage component at the PCC.

$$SI_N(k) = \int_{I_-(k)} i_m(t)\,dt\,. \tag{5}$$

In this way, the following output is computed

$$y(k) = SI_P(k) + SI_N(k)\,. \tag{6}$$

In absence of a DC voltage component during time interval $[kT, (k+1)T]$, the magnetizing current shows a symmetric saturation in intervals $I_-(k)$ and $I_+(k)$, around the zero crossing of the mains voltage. In this case $y(k) = 0$.

On the other hand, in case of a positive voltage bias, the positive semi-period of the flux wave saturates and an asymmetric distortion, which causes even harmonics, appears in the reactor current. The absolute value of SI_P is greater than SI_N (see Fig. 2) and $y(k) > 0$. The sign of $y(k)$ is the same as the DC voltage bias i.e. the DC current component injected into the grid by electric devices connected at the same PCC. In this way, output $y(k)$ plays the role of a DC component detector.

Transfer function (1) shows that the current transformer rejects the DC component. For this reason, the small integral windows, around the grid voltage zero crossing, are mandatory to find the DC voltage component of the grid.

With these premises, a digital dynamic compensation of the offset introduced by the analog conditioning is feasible and the resulting measurement system is free from offset problems. A feedback control can be implemented in order to obtain $y(k) = 0$, that corresponds to a symmetrical saturation of the reactor core and therefore to a null value of the DC voltage component at the PCC. This is obtained injecting into the grid a DC current component that balances the DC current component generated by other loads/power converters connected at the same PCC.

The measured signal $y(k)$ is used to realize, with a simple PI regulator, a closed loop control able to force to zero v_{DC}. Fig. 3 shows the basic idea of the control scheme: the DC component loop produces the set point, i^*_{inv} , for the inner current loop of the power converter.

III. Modeling and Simplified Stability Analysis

A. Simplified model

Fig. 3 outlines the general idea of the compensator's strategy. A more detailed model is presented in Fig. 4, where the converter is composed of a IGBT full bridge with the second-order LC output filter (two inductors L_f and a capacitor C_f with a series resistance R_f) connected to the grid (L_g and R_g represents the distributed parameters of the electric distribution grid). The same figure shows the presence of a generic electric load composed by the inductance L_l, the resistance R_l and the DC generator which causes the DC current flowing towards the grid, i.e. the

equivalent voltage caused by non-linear loads or converters connected along the grid. At the same PCC is connected the non-linear DC voltage component sensor: the reactor.

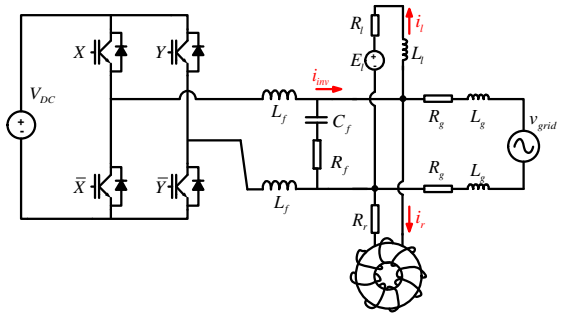

Fig. 4. Schematic of the power circuit.

In order to perform the stability analysis a simpler model was developed. The power converter is usually controlled by a Digital Signal Processor (DSP) which commands the power devices' turn on/off at high frequency in order to limit the harmonic distortion of the output current. The DSP usually embeds a closed loop regulator which can control the output current. The bandwidth of this kind of controller is usually much higher than the considered system (which operates at discrete time at the grid voltage's period), so in the simplified analysis the whole power converter with its output filter can be substituted by an ideal current generator i_{inv}. The grid's distributed inductance L_g presents usually a low value with respect to other inductances, so it can be neglected. The previous assumptions lead to the non-linear model presented in Fig. 5. It is important to note that at this level of simplification the system is still non-linear (the inductance of the reactor is represented by the hysteresis function $\Phi = f(i_r)$).

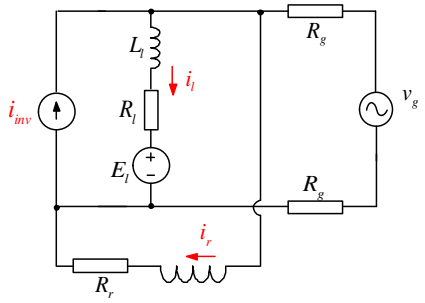

Fig. 5. Simplified non-linear model.

B. Linearized model for stability analysis

The equations of the simplified model, depicted in Fig. 5 are the following

$$\begin{cases} \dot{\Phi}(t) &= v_g(t) - (2R_g + R_r) f^{-1}(\Phi(t)) \\ & \quad +2R_g i_{inv}(t) - 2R_g i_l(t) \\ L_l \dot{i}_l(t) &= v_g(t) - 2R_g f^{-1}(\Phi(t)) - (2R_g + R_l) i_l(t) \\ & \quad +2R_g i_{inv}(t) - E_l(t)\,, \end{cases} \tag{7}$$

where Φ is the reactor flux and i_l the current absorbed by the load. The control input is the inverter current i_{inv}, while E_l, the load equivalent voltage, represents a disturbance. The grid voltage is the periodic signal $v_g = V_g \sin(\omega t)$.

Let $\chi : \mathbb{R} \to \{0, 1\}$ be the indicator function associated to $\mathcal{I}$, the union of intervals $I_-(k)$, $I_+(k)$ (defined by (3)), for all $k \in \mathcal{Z}$, which is, $\forall t \in \mathbb{R}$

$$\chi(t) = \begin{cases} 1 \text{ if } t \in \mathcal{I} \\ 0 \text{ otherwise } . \end{cases}$$

At each sampling time kT the measured output $y(k)$ can then be expressed by the following integral (see also Fig. 2)

$$y(k) = \int_{(k-1)T}^{kT} \chi(t) i_m(t) dt\,, \tag{8}$$

where the measured current i_m satisfies the following first order differential equation (see (2))

$$\frac{di_m(t)}{dt} = \frac{df^{-1}}{d\phi(t)}|_{\Phi(t)} \frac{d\Phi}{dt} - p\, i_m(t)\,. \tag{9}$$

Augmented system (7)+(9) is rewritten as

$$\dot{x} = F(x, t, E_l, i_{inv})\,, \tag{10}$$

where $x = (\Phi,\, i,\, i_m)^T$.

System (7)+(9) is asymptotically stable since it models an electric system composed of passive components. In nominal conditions, i.e. when no disturbance is applied ($E_l = 0$) and the inverter current is null ($i_{inv} = 0$), the state x asymptotically converges to a $\frac{2\pi}{\omega}$-periodic signals $x_0 = (\Phi_0, i_{l0}, i_{mo})$ which satisfies

$$\dot{x}_0(t) = F(x_0(t), t, 0, 0)\,. \tag{11}$$

To study the behavior of system (10) in a neighborhood of the reference solution x_0, we set the error vector $e = x - x_0$, with components $e = (e_\phi, e_{i_l}, e_{i_m})$. Then, by (10) and (11)

$$\dot{e} = G(e, t, E_l, i_{inv})\,,$$

where $G(e, t, E_l, i_{inv}) = F(x_0 + e, t, E_l, i_{inv}) - F(x_0, t, 0, 0)$. The corresponding linearized model in a neighborhood of the equilibrium $e = (0, 0, 0)$ is the time-varying system

$$\dot{e} = A(\omega t)e + B i_{inv} + W E_l\,, \tag{12}$$

where, setting $\alpha(t) = \frac{df^{-1}}{d\Phi}|_{\Phi_0(t)}$

$$A(t) = \frac{d}{de} G(e, t, E_l, i_l)|_{e=0, E_l=0, i_{inv}=0} = \begin{pmatrix} -(2R_g + R_r)\alpha(t) & -2R_g & 0 \\ -2\frac{R_g}{L_l}\alpha(t) & -\frac{2R_g + R_l}{L_l} & 0 \\ -(2R_g + R_r)\alpha^2(t) & -2R_g\alpha(t) & -p \end{pmatrix},$$

$$B = \frac{dG}{dI_{inv}} = \begin{pmatrix} 2R_g \\ 2\frac{R_g}{L_l} \\ 2R_g\alpha(t) \end{pmatrix}, \; W = \frac{dG}{dE_l} = \begin{pmatrix} 0 \\ -2\frac{R_g}{L_l} \\ 0 \end{pmatrix}.$$

In this system, i_{inv} is the control input and E_l represents a disturbance.

Using the method presented in section (II), the control variable i_{inv} is obtained through a first order hold filter applied to the output of a discrete-time controller. Since i_{inv} is constant in time intervals $[kT, (k+1)T]$, the error e satisfies the difference equation obtained by discretizing (12) through a first-order hold:

$$e(T(k+1)) = A_T e(Tk) + B_T i_{inv}(Tk) + W_T(k)\,, \tag{13}$$

where $A_T = \Psi(T)$, $B_T = \int_0^T \Psi(T)\Psi^{-1}(\tau)Bd\tau$, $W_T(k) = \int_0^T \Psi(T)\Psi^{-1}(\tau)WE_l(kT+\tau)d\tau$ and Ψ is the transition matrix associated to system (12), that is it is the solution of

$$\begin{cases} \dot{\Psi}(t) = A(t)\Psi(t) \\ \Psi(0) = I\,. \end{cases}$$

The measured signal is given by (8).

Remark that, in nominal conditions, signal i_m is symmetric). Therefore, if $y_0(k)$ represents the output in nominal conditions

$$y_0(k) = \int_{kT}^{(k+1)T} \chi(t) i_{m0}(t)dt = 0\,,$$

Since $i_m = i_{m0} + e_{i_m}$, $e_{i_m}(t+KT) = (0,0,1)\Psi(t)e(KT)$, the linearized output is given by

$$y(k) = C_T e(Tk) \tag{14}$$

where $C_T = \int_{kT}^{(k+1)T} \chi(t)(0,0,1)\Psi(t)dt$.

The discrete-time PI controller is given by

$$\begin{cases} i_{inv}(k) = k_p y(k) + k_i s(k) \\ s(k+1) = s(k) + y(k)\,. \end{cases} \tag{15}$$

In general, the parameters k_p, k_i appearing in (15) can be designed using the reduced linear discrete-time model (13) + (14) + (15) and stability can be checked by computing the eigenvalues of the closed loop system.

In the following we present a simplified analysis of stability.

C. A simplified stability analysis

If parameter L_l appearing in (12) is small enough, it is possible to use singular perturbation theory to reduce the model (see [12]).

In this hypothesis, the dynamic of state e_{i_l} can be considered a fast-dynamic which converges rapidly to the value

$$e_{i_k}(t) = -\frac{2R_g}{2R_g+R_l}\alpha(t)e_\phi - \frac{2R_g}{2R_g+R_l}(I_{inv} - E_l)\,.$$

The slow component of the state is $e_s = (e_\Phi, e_{i_m})$ and its reduced equations are given by

$$\dot{e}_s(t) = A_0(t)e_s(t) + B_0 i_{inv}(t) + W_0 E_l(t)\,, \tag{16}$$

setting $c_1 = \frac{2R_g(R_l+R_r)+R_rR_l}{2R_g+R_l}$, $c_2 = 2R_g + \frac{4R_g^2}{2R_g+R_l}$, $c_3 = \frac{4R_g^2}{2R_g+R_l}$ the matrices appearing in (16) are given by

$$A_0(t) = \begin{pmatrix} -c_1\alpha(t) & 0 \\ -c_1\alpha^2(t) & -p \end{pmatrix}\,,$$

$$B_0(t) = \begin{pmatrix} c_2 \\ \alpha(t)c_2 \end{pmatrix}\,,$$

$$W_0(t) = \begin{pmatrix} -c_3 \\ -\alpha(t)c_3 \end{pmatrix}\,.$$

Let Ψ_0 be the solution of

$$\begin{cases} \dot{\Psi}_0(t) = A_0(t)\Psi_0(t) \\ \Psi_0(0) = I\,, \end{cases}$$

if the eigenvalues of matrix A_0 are small compared to $\frac{2\pi}{T}$, it is possible to approximate Ψ_0 in the following way

$$\Psi_0(t) \simeq I + \int_0^t A(\tau)d\tau\,.$$

With this approximation, discretizing system (16) with a zero-order hold we obtain

$$e((k+1)T) = A_{T0}e(kT) + B_{T0}i_{inv}(kT) + W_{T0}E_l(kT)\,,$$

setting $\bar{\alpha} = \frac{1}{T}\int_0^T \alpha(t)dt$, the system matrices are given by

$$A_{T0} = I + T\begin{pmatrix} -c_1\bar{\alpha} & 0 \\ -c_1\bar{\alpha}^2 & -p \end{pmatrix}\,,$$

$$B_{T0} = T\begin{pmatrix} c_2 \\ \bar{\alpha}c_2 \end{pmatrix}\,,$$

$$W_{T0} = T\begin{pmatrix} -c_3 \\ -\bar{\alpha}c_3 \end{pmatrix}\,.$$

The measured output (8) is approximated by

$$\begin{aligned} y(k) &= \int_0^T \chi(t)((0,1)A_0(t)e(kT) + B_0(t)i_{inv}(kT))dt \\ &= (-c_1\hat{\alpha}^2, -\hat{p})e(kT) + c_2\hat{\alpha}i_{inv}(kT) - c_3\hat{\alpha}E_l\,, \end{aligned}$$

where $\hat{\alpha} = \int_0^T \chi(t)\alpha(t)dt$ and $\hat{p} = \int_0^T \chi(t)p(t)dt$.

To define the PI controller, we add an integrator to the system output, the value of the integrator is represented by state s

$$s(k) = s(k-1) + y(k-1); \tag{17}$$

in this way the control input is given by

$$i_{inv} = -k_p y(k) - k_i s(k)\,.$$

Let the state of (16)+(17) be given by $z(k) = (e^T(k), s(k))$, then $z(k+1) = A_{k_p,k_i}z(k)$, where matrix A_{k_p,k_i} depends on gains k_p, k_i.

If $k_p = 0$, $k_i = 0$ then

$$A_{0,0} = \begin{pmatrix} 1-\bar{\alpha}c_1 & 0 & 0 \\ -\bar{\alpha}^2 c_1 & 1-p & 0 \\ -\hat{\alpha}c_1 & -\hat{p} & 1 \end{pmatrix}$$

the associated eigenvalues are $\{1-\bar{\alpha}c_1, 1-p, 1\}$. We prove that the system is stabilized for sufficiently small gains k_p, k_i. In fact the first 3 eigenvalues are stable and, by continuity, remain stable for small values of k_p and k_i. Using perturbation theory, assume that $k_p = 0$ and k_i is a small constant. In this case

$$A_{0,k_i} - A_{0,0} = k_i\begin{pmatrix} 0 & 0 & c_2 \\ 0 & 0 & \bar{\alpha}c_2 \\ 0 & 0 & \hat{\alpha}c_2 \end{pmatrix} = k_i\bar{A}$$

let x_1 and y_1 be respectively the right and left eigenvectors of matrix $A_{0,0}$ for eigenvalue 1 and let $\lambda(k_i)$ be the value of the largest eigenvalue of A_{0,k_i} as a function of k_i (hence $\lambda(0) = 1$), where

$$x_1 = (0,0,1)^t\,,$$

$$y_1 = (\frac{\hat{p}\bar{\alpha}^2 + \hat{\alpha}p}{\bar{\alpha}p}, -\frac{\hat{p}}{p}, 1)\,,$$

using expression (9.4) from chapter 2 of [13], the derivative of the eigenvalue 1 with respect to parameter k is given by

$$\lambda'(0) = \frac{y_1^T \bar{A} x_1}{y_1^T x_1} = -\frac{\hat{\alpha} c_2 (\bar{\alpha} + 1)}{\bar{\alpha}} .$$

since the quantities $\hat{\alpha}$, c_2, $\bar{\alpha}$ are positive, $\lambda'(0)$ is negative, this shows that for small values of k_p the closed loop system is asymptotically stable, since the eigenvalue in 1 is moved in negative direction, towards the interior of the unit circle.

Finally, the steady state error due to a constant disturbance E_l to the flux Φ is null since by direct computation it can be verified that the static gain from E_l to e_Φ is 0.

IV. Simulations and Model Validation

The aforementioned compensation strategy was simulated in a Matlab/Simulink environment with the aid of PLECS, a Simulink toolbox which allows fast simulation of electronic converters with feedback controls. In order to validate the reduced model (13), presented in Section III-A, a Simulink model closest to the real-world realization was implemented. In particular, the block scheme in Fig. 3 was simulated, Fig. 4 shows in details the circuit used for simulations. The parameters were $V_{DC} = 450V$, $L_f = 1.2mH$, $R_f = 1\Omega$, $C_f = 2.2\mu F$, $R_g = 0.2\Omega$, $L_g = 40\mu F$, $V_g = 230V_{RMS}$, $T = 20ms$, $E_l = 1V$, $R_l = 10\Omega$, $R_r = 29\Omega$, $L_l = 1mH$.

The signal processing was done at discrete time (sampling frequency $F_{sw} = 10kHz$) with 16-bit numeric variables (in order to match the processing capabilities of a low-cost DSP). The block *DC Component detection* in Fig. 3 was implemented filtering the reactor current with a first-order high-pass filter (cut frequency $100rad/s$) to account for the transfer function of the current transformer used for the current measurement, and the resulting waveform (measured magnetizing current, with reference to Fig. 2) was integrated in a window of 20 samples ($\Delta T_{ZC} = 1ms$) centered in the grid voltage's zero-crossing.

The $CurrentController$ was a discrete PI regulator ($k_p = 0.08$, $k_i = 306E-6$, sampling time $100\mu s$). The same structure (PI regulator) was chosen also for the compensator ($k_p = 151$, $k_i = 4557$, sampling time $20ms$).

The model realized should approximate with a good degree of accuracy a real full-bridge converter driven by a fixed-point DSP controller which implements the proposed compensation strategy. To validate the simplified model various simulation were performed comparing its results with the complete model. The results were quite good, despite the high number of assumptions that led to the simplified discrete-time linear model. In particular, Fig. 6 shows the mean reactor current i_{R_DC} when a disturbance $E_l = 1V$ was inserted at the time $0.2s$. Furthermore, Fig. 7(a) and 7(b) show the transients of i_{R_DC} and the inverter current i_{inv} with the same perturbation but with the compensator active. The top waveforms are the output of the complete model, while the bottom waveforms refer to the simplified model.

As it is evident, the results are in good agreement, regarding numerical values and transient time.

V. Experimental Results

A picture of the prototype is presented in Fig. 8(a). It was based on a Freescale MC56F8323 DSP that performed the proposed strategy and on a three-level PWM modulation with a switching frequency equal to $10kHz$. The power converter

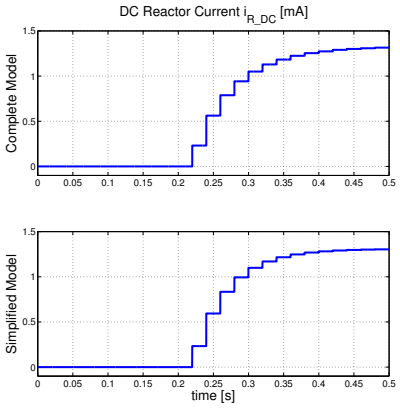

Fig. 6. Comparison between the complete model DC reactor current i_{R_DC} (top waveforms) and the simplified ones (bottom waveforms) without the compensator.

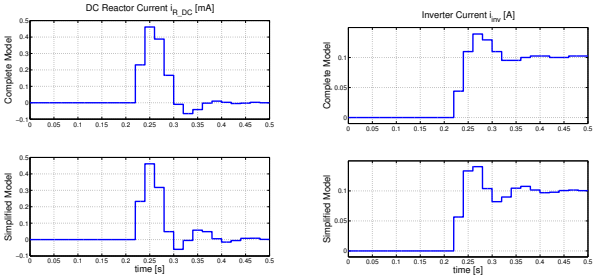

(a) DC reactor current i_{R_DC}. (b) Inverter current i_{inv}.

Fig. 7. Comparison between the complete model (top waveforms) and the simplified one (bottom waveforms).

was connected to the grid by a simple LC filter relying on two $1.2mH$ inductors and on a $1.5\mu F$ capacitor. Fig. 8(b) shows the DC voltage sensing circuit. A cheap magnetic component was used for the reactor: the core material was Fe-Si, generally used for cheap line frequency transformers, and the parasitic winding resistance was 29Ω. This high value of resistance is caused by the high number of turns (2950) and the small wire diameter ($0.315mm$). A simple current transformer was used to realize a measure of the reactor current free from offset problems.

To test the effectiveness of the proposed solution a low voltage test bed was realized: the setup is presented in Fig. 9. The PCC was the output of a power transformer, which lowered the grid voltage from $230V_{RMS}$ to $26VRMS$. The

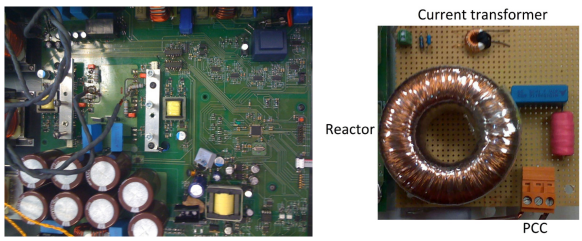

(a) Power converter. (b) DC sensor.

Fig. 8. Picture of the power converter and of the DC voltage sensing circuit used for the experimental results.

equivalent schematic accounts also the series impedance of the real transformer and of the grid, Z_{grid_2}. The firmware on-board the DSP controlled also the active power to obtain a DC-Link voltage of $110V$. At the PCC a non-linear load (a 20Ω power resistance with a series diode) was connected. The control of the DC-Link voltage was realized by absorbing active power from the grid in order to charge the DC capacitors of the power converter. The output current of the active filter will be the superposition of a sinusoidal supply current and the DC current needed to compensate the non-linear distortion at the PCC. Without the use of the proposed solution a significant DC current component of $580mA$ was present at the PCC. The effect of this non-linear load (diode + resistance) on the current flowing at the input of the transformer, I_{grid_1}, is shown in Fig. 10(a), where it is evident that the transformer core was heavily saturated and, as a consequence, it drained a very distorted current from the grid. Fig. 10(b) shows also the transformer secondary current, which presents the typical characteristic of the half-cycle rectifier.

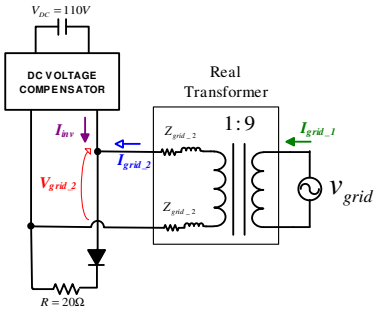

Fig. 9. Schematic of the low voltage test bed.

On the contrary, with the compensating system connected, the converter, in addition to the active current needed to compensate for its own power consumption, injected a direct current component, which fully compensated the DC current component previously absorbed from the output of the transformer. Fig. 11 shows the output voltage and current of the transformer (I_{grid_2} and V_{grid_2}) with the DC voltage compensator ON. The same figure shows also the DC current component of I_{inv} that is about $-600mA$ (green trace), i.e. the DC current component caused by the non-linear load alone.

A precise DC current meter used for the measurement of the actual DC current component of I_{grid_2} showed only a small oscillation of mA around zero, i.e. the precision of the instrument.

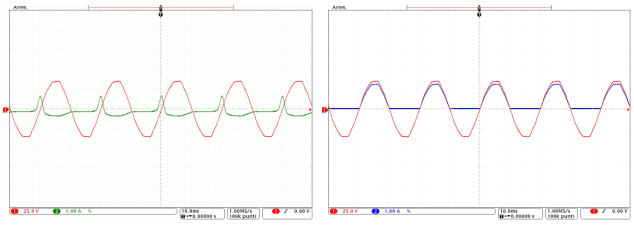

(a) V_{grid_2} and I_{grid_1}. (b) V_{grid_2} and I_{grid_2}.

Fig. 10. Transformer voltage (red trace) and currents (green and blue traces) without DC voltage compensator.

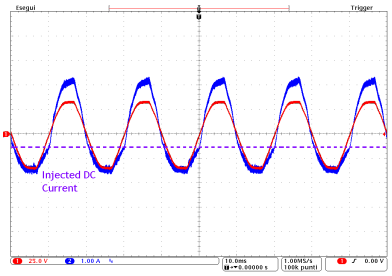

Fig. 11. Transformer voltage V_{grid_2} (red trace) and current I_{grid_2} (blue trace) in presence of a diode + resistive load. DC voltage compensator On.

VI. Conclusions

This paper proposed a non-linear sensor and a grid connected system that act as an active filter to remove the DC current component flowing in the power lines, that could potentially damage the distribution power transformers. A simplified model of the real system was realized and a mathematical analysis was performed, pointing out that the system can be always rendered asymptotically stable by an appropriate choice of the compensator's parameters. Simulation results confronting the simplified, discrete-time, linear model and the complete, continuous-time, non-linear model showed that the simplified model closely approximated the other model's behavior. Finally, experimental results showed the ability of the proposed strategy to effectively compensate the DC current caused by non-linear loads connected at the PCC.

References

[1] V. Salas, E. Olias, M. Alonso, F. Chenlo, and A. Barrado, "Dc current injection into the network from pv grid inverters," in *Photovoltaic Energy Conversion, Conference Record of the 2006 IEEE 4th World Conference on*, vol. 2, may. 2006, pp. 2371 –2374.

[2] L. Gertmar, P. Karlsson, and O. Samuelsson, "On dc injection to ac grids from distributed generation," in *Power Electronics and Applications, 2005 European Conference on*, 2005, pp. 10 pp. –P.10.

[3] D. Infield, P. Onions, A. Simmons, and G. Smith, "Power quality from multiple grid-connected single-phase inverters," *Power Delivery, IEEE Transactions on*, vol. 19, no. 4, pp. 1983 – 1989, oct. 2004.

[4] D. Warner and W. Jewell, "An investigation of zero order harmonics in power transformers," *Power Delivery, IEEE Transactions on*, vol. 14, no. 3, pp. 972 –977, July 1999.

[5] P. Picher, L. Bolduc, A. Dutil, and V. Pham, "Study of the acceptable dc current limit in core-form power transformers," *Power Delivery, IEEE Transactions on*, vol. 12, no. 1, pp. 257 –265, Jan. 1997.

[6] N. Takasu, T. Oshi, F. Miyawaki, S. Saito, and Y. Fujiwara, "An experimental analysis of dc excitation of transformers by geomagnetically induced currents," *Power Delivery, IEEE Transactions on*, vol. 9, no. 2, pp. 1173 –1182, Apr. 1994.

[7] S. Lu and Y. Liu, "Fem analysis of dc saturation to assess transformer susceptibility to geomagnetically induced currents," *Power Delivery, IEEE Transactions on*, vol. 8, no. 3, pp. 1367 –1376, July 1993.

[8] G. Buticchi, G. Franceschini, E. Lorenzani, C. Tassoni, and A. Bellini, "A novel current sensing dc offset compensation strategy in transformerless grid connected power converters," in *Energy Conversion Congress and Exposition, 2009. ECCE 2009. IEEE*, sep. 2009, pp. 3889 –3894.

[9] G. Franceschini, E. Lorenzani, A. Bellini, and A. Fratta, "Compensation of magnetic core saturation for grid connected single-phase power converters," in *ICEM 2010. IEEE*, sep. 2010, pp. 1 – 6.

[10] F. Wang, J. Zhang, Z. Jin, Y. Cao, D. He, and C. Xu, "Experimental study of the effects of dc-bias current on the power transformer," in *Power and Energy Engineering Conference (APPEEC), 2010 Asia-Pacific*, mar. 2010, pp. 1 –4.

[11] G. Buticchi, L. Consolini, and E. Lorenzani, "A nonlinear reactor for dc current compensation in single phase power lines," in *IFAC World Congress 2011*, Aug 2011 - to appear.

[12] P. Kokotovic, H. Khalil, and J. O'Reilly, *Singular Perturbation Methods in Control, Analysis and Design*. SIAM, 1999.

[13] J. H. Wilkinson, *The Algebraic Eigenvalue Problem*. Clarendon Press, Oxford, 1965.